Deep-Inelastic e^+p Scattering at Very High Q^2 from ZEUS at HERA

C.M. Ginsburg
The Ohio State University, Physics Department, Columbus, OH 43210-1106, USA
on behalf of the ZEUS Collaboration

Neutral-current and charged-current deep-inelastic scattering at very high four-momentum transfer squared (Q^2) have been studied in positron-proton collisions at center-of-mass energy 300 GeV using the ZEUS detector at HERA. An integrated luminosity of 47.7 pb^{-1} was collected in the years 1994-1997. Differential cross sections are presented for $Q^2 > 400$ GeV^2 and compared to Standard Model predictions.

I. DEEP-INELASTIC SCATTERING AT HERA

Deep-inelastic scattering (DIS) provides a wealth of information about nucleon structure. Recently, very high momentum transfers in DIS have been achieved at the HERA collider, where 820 GeV protons have been collided with 27.5 GeV positrons for a center-of-mass energy $\sqrt{s}$=300 GeV. In the highest momentum transfer region, e^+p DIS cross sections depend on proton parton densities and properties of the electroweak interaction.

The $e^\pm p$ DIS process is illustrated in Fig. 1. The variables used to describe the process are x, the struck parton momentumfraction, y, the fractional energy transfer in the proton rest frame (inelasticity) and Q^2, the four-momentum transfer squared, where $Q^2 = sxy$. Neutral-current DIS events are characterized by the exchange of a photon or Z-boson, and have a positron and a jet (or jets) in the final state. The outgoing positron and the hadronic matter are balanced in transverse momentum. Charged-current DIS events are characterized by the exchange of a W-boson, and contain an undetected neutrino and a jet (or jets) in the final state. The presence of the neutrino is detected as missing transverse momentum.

The DIS data presented here were collected and analyzed by the ZEUS collaboration and correspond to an integrated luminosity of 47.7 pb^{-1} taken from 1994 to 1997.

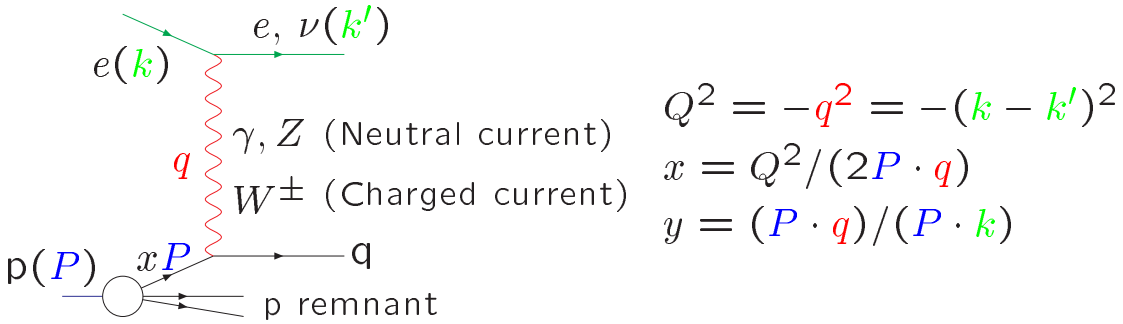

FIG. 1. The $e^\pm p$ deep-inelastic scattering process.

II. THE ZEUS DETECTOR

ZEUS [1] is a multi-purpose magnetic detector; the primary components used in these analyses are the calorimeters (RCAL,BCAL,FCAL), the central tracking detector (CTD), and the luminosity monitor. The coordinate system is defined such that the z-axis follows the proton direction, and the origin is the nominal ep interaction point. The ZEUS detector is displayed in Fig. 2.

The ZEUS compensating uranium-scintillator calorimeter covers the polar angle region $2.6° < \theta < 176.1°$ with full azimuthal coverage over this region. Its energy resolution for electromagnetic showers is $\sigma_E/E \simeq 18\%/\sqrt{E(\mathrm{GeV})}$,

and for hadronic showers is $\sigma_E/E \simeq 35\%/\sqrt{E(\mathrm{GeV})}$, as measured under test-beam conditions.

The ZEUS CTD operates in a solenoidal 1.43 T magnetic field, and primarily provides vertex reconstruction, track momentum, and charge information for these analyses.

The luminosity is determined from the rate of Bethe-Heitler bremsstrahlung ($ep \to ep\gamma$) photons detected in an electromagnetic calorimeter at $z = -107$ m.

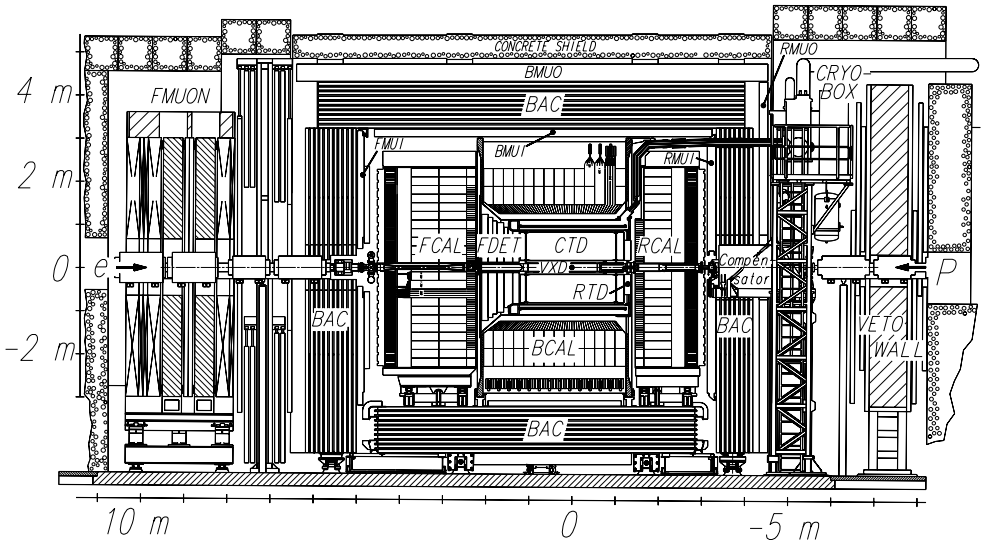

FIG. 2. The ZEUS detector.

III. STRUCTURE FUNCTION FORMALISM

To lowest order (QED Born level) the neutral-current DIS ($e^+p \to e^+X$) cross section is

$$\frac{d^2\sigma^{NC}(e^+)}{dx\,dQ^2} = \frac{2\pi\alpha^2}{xQ^4}\left[Y_+\,\mathcal{F}_2^{NC}(x,Q^2) - Y_-\,x\mathcal{F}_3^{NC}(x,Q^2) - y^2\,\mathcal{F}_L^{NC}(x,Q^2)\right] \tag{1}$$

where $Y_\pm = 1 \pm (1-y)^2$. In lowest-order QCD, the structure functions $\mathcal{F}_2^{NC}$ and $x\mathcal{F}_3^{NC}$ are the sums over quark flavor of the product of quark couplings and momentum distributions. The quark couplings depend on the quark charges, and the electroweak parameters M_Z, $\sin^2\theta_W$, etc.

The QED Born-level charged-current DIS ($e^+p \to \bar{\nu}_e X$) cross section is

$$\frac{d^2\sigma^{CC}(e^+)}{dx\,dQ^2} = \frac{G_F^2}{4\pi x}\left(\frac{M_W^2}{Q^2+M_W^2}\right)^2\left[Y_+\,\mathcal{F}_2^{CC}(x,Q^2) - Y_-\,x\mathcal{F}_3^{CC}(x,Q^2) - y^2\,\mathcal{F}_L^{CC}(x,Q^2)\right] \tag{2}$$

where at lowest order the structure functions $\mathcal{F}_2^{CC}$ and $x\mathcal{F}_3^{CC}$ contain sums and differences of quark and antiquark momentum distributions.

The neutral- and charged-current longitudinal structure functions, $\mathcal{F}_L^{NC}$ and $\mathcal{F}_L^{CC}$, respectively, provide a small ($\sim 1\%$) contribution in the kinematic range discussed here, and have been included.

Electroweak radiative corrections to these Born-level equations, including initial- and final-state radiation, vertex and propagator corrections, and two-boson exchange, are significant and have been included to at least lowest order [2].

IV. THE VERY HIGH-Q^2 NEUTRAL-CURRENT AND CHARGED-CURRENT DATA

The differential NC DIS cross section $d\sigma^{NC}/dQ^2$ is shown in Fig. 3; $d\sigma^{NC}/dx$ and $d\sigma^{NC}/dy$ are shown in Fig. 4. The differential CC DIS cross sections $d\sigma^{CC}/dQ^2$, $d\sigma^{CC}/dx$, and $d\sigma^{CC}/dy$, are shown in Figs. 5, 6. and 7, respectively.

For both neutral and charged current, the data points are compared to the Standard Model predictions using the CTEQ4D [3] parton distribution functions (PDF's), shown by the solid curves, with estimated PDF uncertainty shown by the shaded bands.

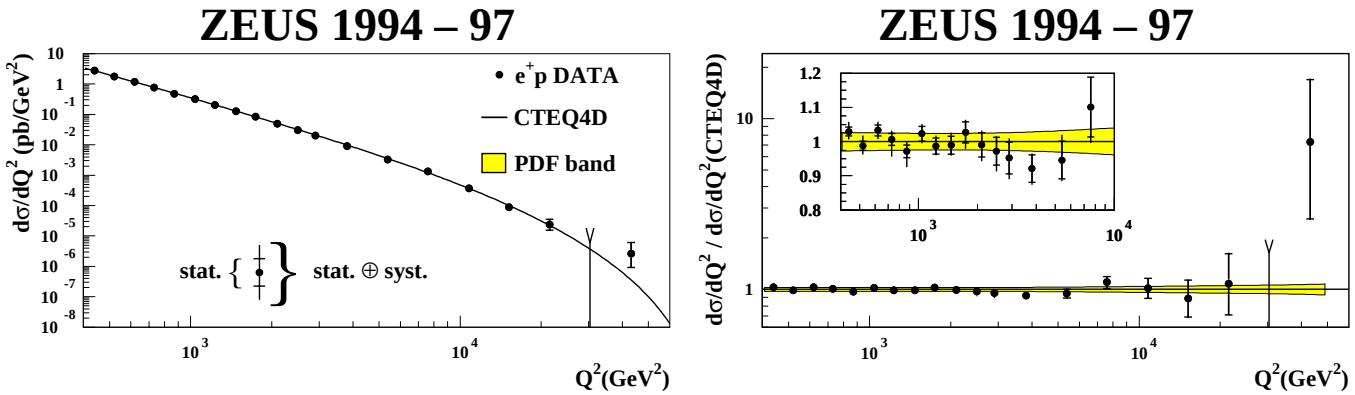

FIG. 3. The neutral-current DIS (a) differential cross section $d\sigma/dQ^2$, and (b) ratio of data to SM prediction with blow-up view of $400 < Q^2 < 10000$ GeV^2 region (inlaid).

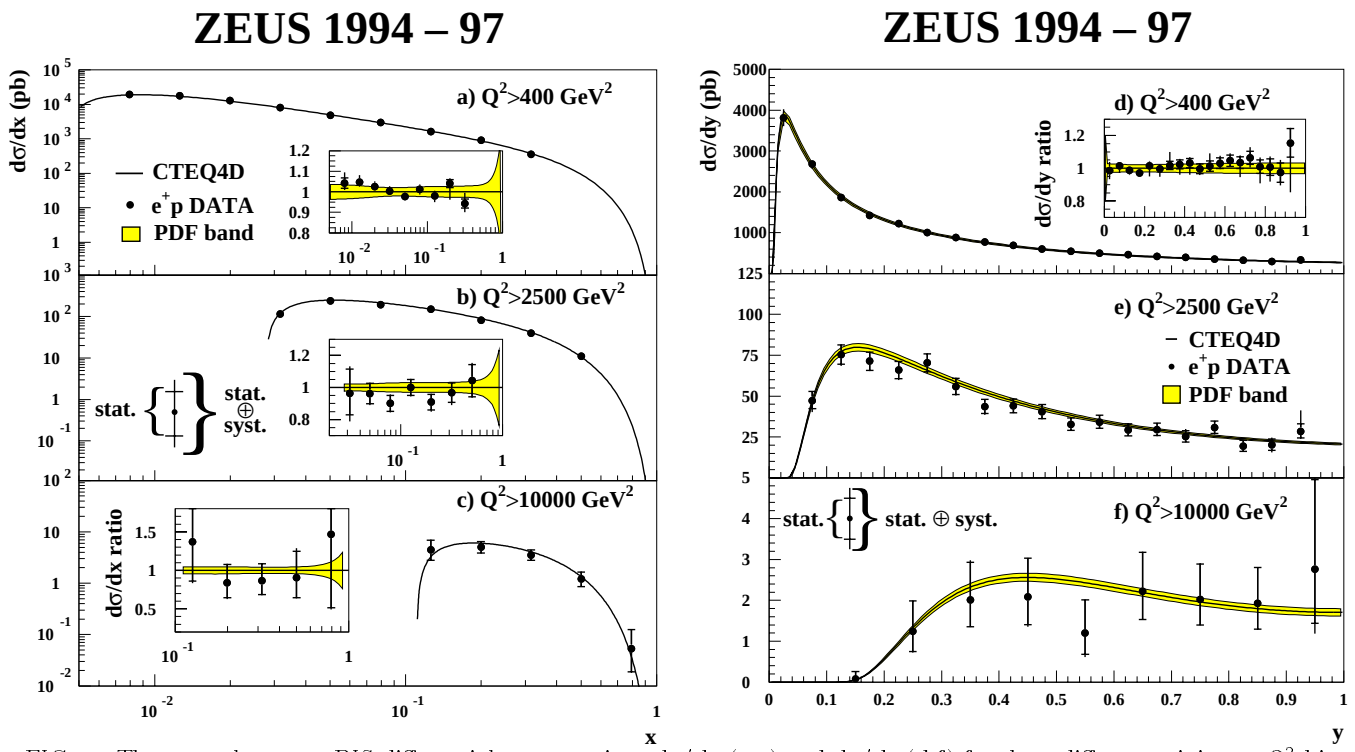

FIG. 4. The neutral-current DIS differential cross sections $d\sigma/dx$ (a-c) and $d\sigma/dy$ (d-f) for three different minimum-Q^2 bins: (a,d) $Q^2 > 400$ GeV, (b,e) $Q^2 > 2500$ GeV, and (c,f) $Q^2 > 10000$ GeV. The inlaid plots show the ratio of the data to the Standard Model prediction.

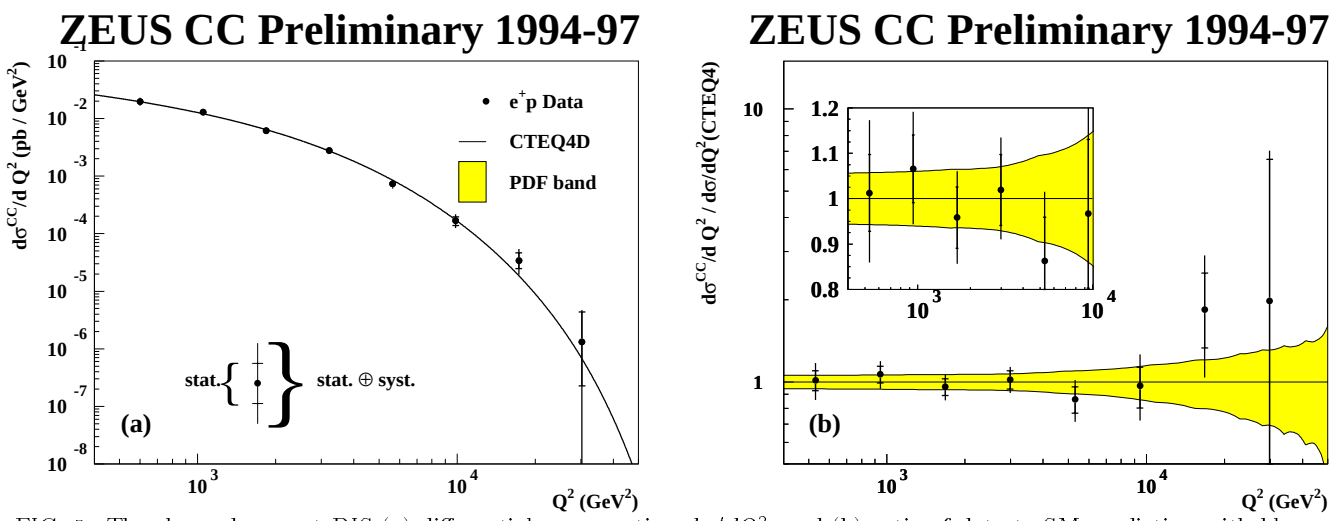

FIG. 5. The charged-current DIS (a) differential cross section $d\sigma/dQ^2$, and (b) ratio of data to SM prediction with blow-up view of $400 < Q^2 < 10000$ GeV^2 region (inlaid).

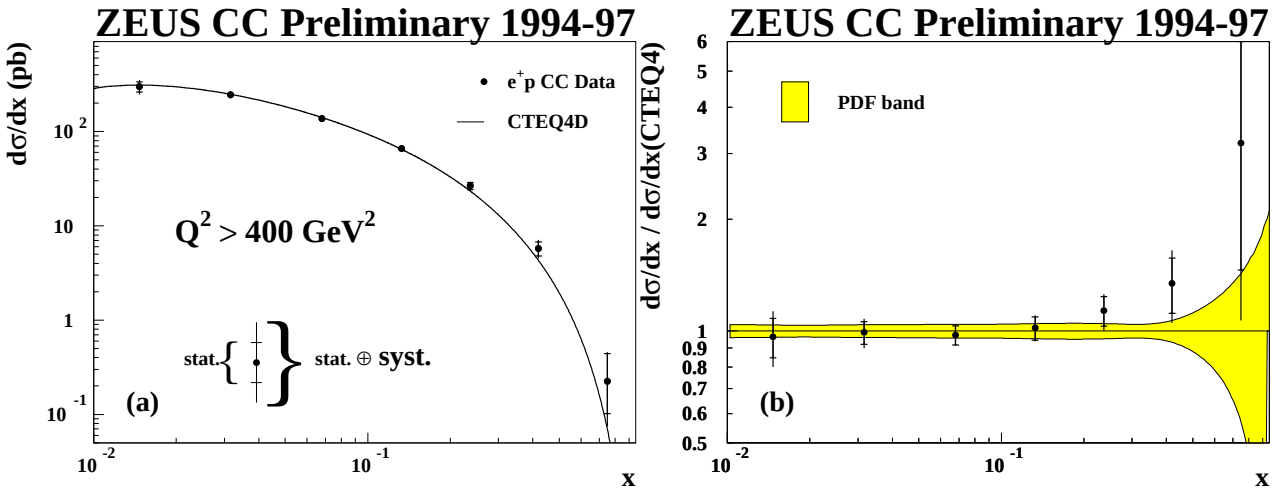

FIG. 6. The charged-current DIS (a) differential cross section $d\sigma/dx$, (b) ratio of data to SM prediction.

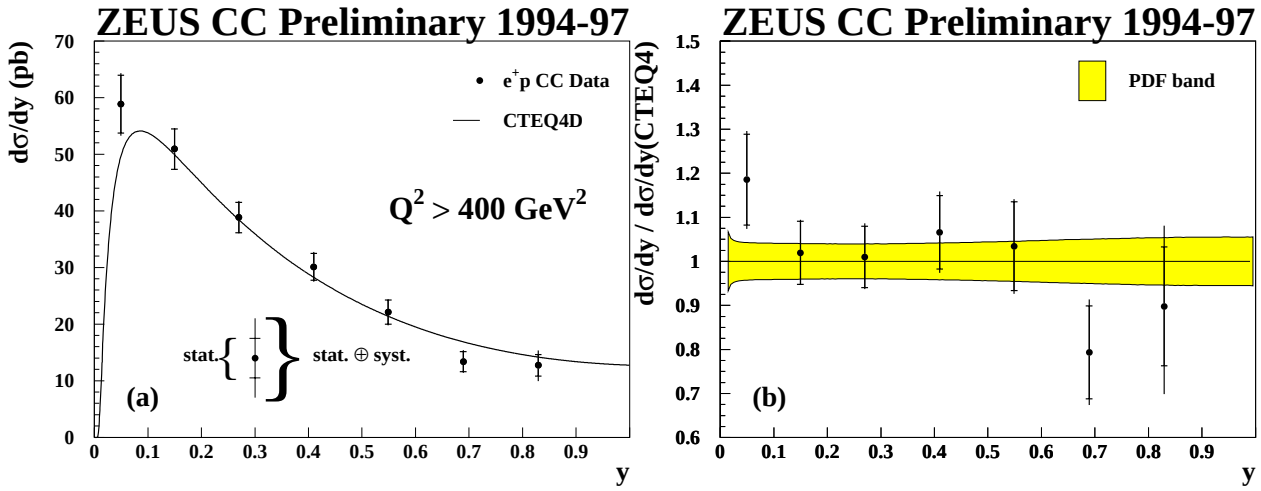

FIG. 7. The charged-current DIS (a) differential cross section $d\sigma/dy$, and (b) ratio of data to SM prediction.

The PDF uncertainty is calculated from a NLO fit [4] to world DIS data, and includes statistical and systematic errors on these data, as well as variations in the assumed electroweak and QCD parameters. For the neutral-current cross section, these uncertainties range from 2.5% at $Q^2 = 400$ GeV^2 to 8% at $Q^2 = 40000$ GeV^2. For the charged-current cross section, the extracted uncertainties range from 9% at $Q^2 = 400$ GeV^2 to 17% at $Q^2 = 10000$ GeV^2. The larger CC uncertainty is due to the larger uncertainty in the d-quark PDF relative to the u-quark PDF. Both the NLO fit, which includes higher-twist effects, and a recent reanalysis of NMC and SLAC data [5] yield a larger d/u ratio at high-x than the CTEQ4 PDF's, where the d/u ratio is constrained to be zero at $x = 1$. Within present experimental precision, any of these hypotheses can be accommodated; their differences are not included in the PDF uncertainty band. Increasing the d/u ratio at high-x reduces the CC data excess at high-x, but does not appreciably affect the NC cross section since the NC process is not sensitive to the d-quark.

The charged-current DIS reduced cross section

$$\tilde{\sigma} = \frac{d^2\sigma}{dx\,dQ^2} \cdot \frac{2\pi x}{G_F^2} \cdot \left(\frac{M_W^2}{Q^2 + M_W^2} \right)^{-2} = x(\bar{u} + \bar{c}) + x(1-y)^2(d+s) \tag{3}$$

is shown in Fig. 8 along with the Standard Model (CTEQ4D) prediction. At high-x, the valence d and s quarks (dashed curves) dominate $\tilde{\sigma}$, whereas at lower-x the $\bar{u}$ and $\bar{c}$ sea quarks (dotted curves) dominate.

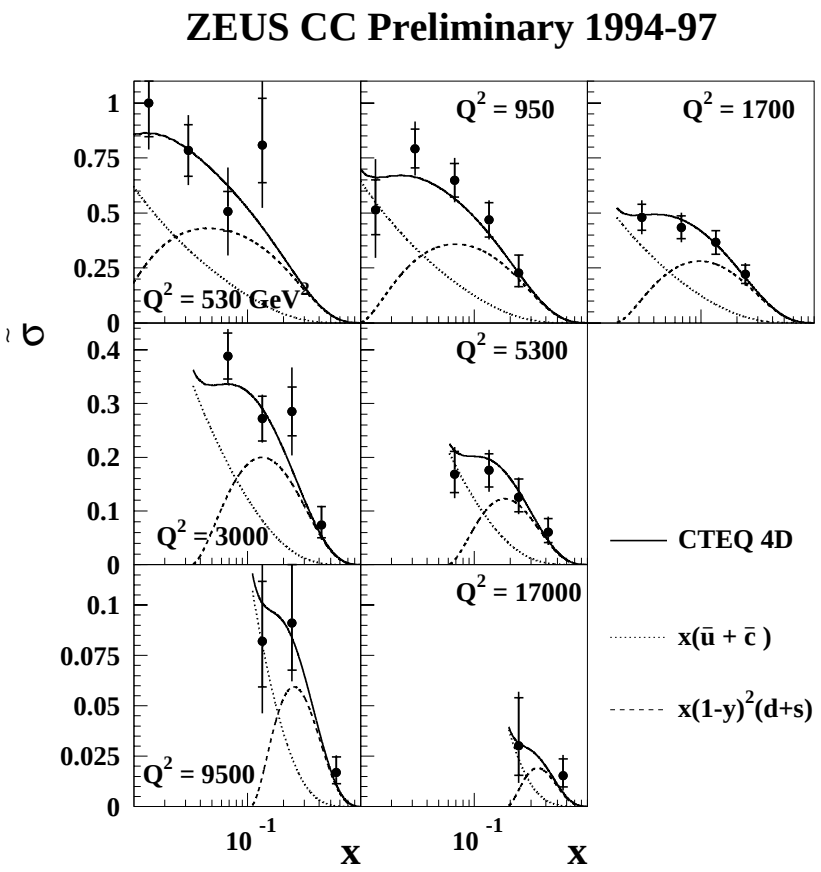

FIG. 8. The charged-current DIS reduced cross section data as a function of x in bins of Q^2, compared to the Standard Model predictions.

At momentum-transfer-squared close to the Z and W masses squared, i.e., $Q^2 \gtrsim 6000 - 8000$ GeV^2, the cross sections become sensitive to contributions from these exchanges, and to the propagator masses in particular.

The sensitivity of the NC cross section to the Z mass is demonstrated in Fig. 9. The measured cross sections are compared with the Standard Model predictions by varying M_Z while keeping the couplings fixed. Three mass values

are considered, $M_Z = 40$, 91 and ∞ GeV. Clearly, $M_Z \sim 91$ GeV is favored, in agreement with the world average value $M_Z = (91.187 \pm 0.007)$ GeV [6].

In the CC channel, the sensitivity of the cross section to the W mass is better than in the NC case, as shown in Fig. 10. The M_W may be extracted by a χ^2 fit to the measured cross sections, leaving all other electroweak parameters fixed, with the result

$$M_W = 78.6^{+2.5}_{-2.4}(\text{stat.})^{+3.3}_{-3.1}(\text{syst.})\ \text{GeV}. \tag{4}$$

This may be compared with the world average value of $M_W = (80.41 \pm 0.10)$ GeV [6].

The agreement between these Z and W masses and the masses extracted through timelike production in e^+e^- and $\bar{p}p$ data confirms the Standard Model prediction in the spacelike regime.

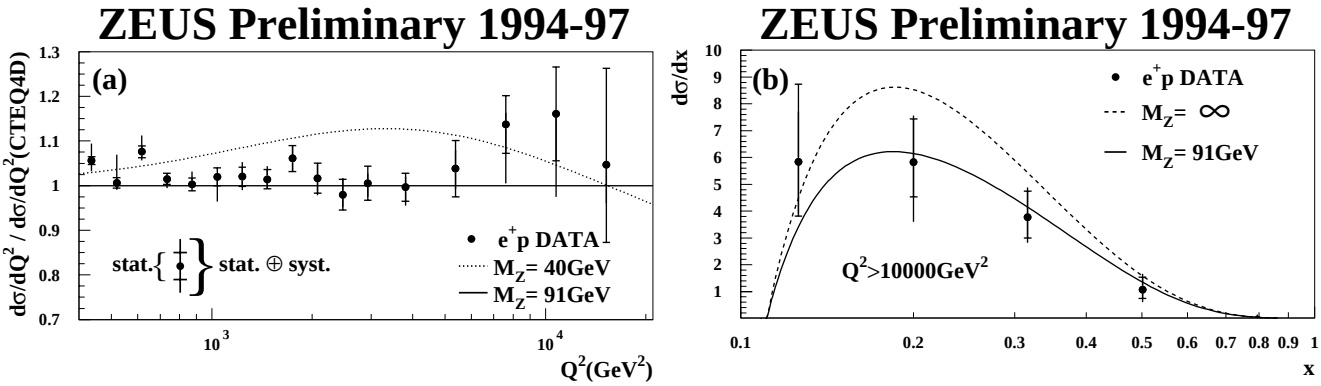

FIG. 9. Sensitivity of the NC cross section to the Z mass: (a) the ratio of NC differential cross section $d\sigma/dQ^2$ to the SM prediction (solid line), and with the assumption of $M_Z = 40$ GeV (dashed curve); and (b) the $Q^2 > 10000$ GeV^2 NC differential cross section $d\sigma/dx$ compared to the SM prediction (solid curve), and with the assumption of an infinite Z mass (dashed curve).

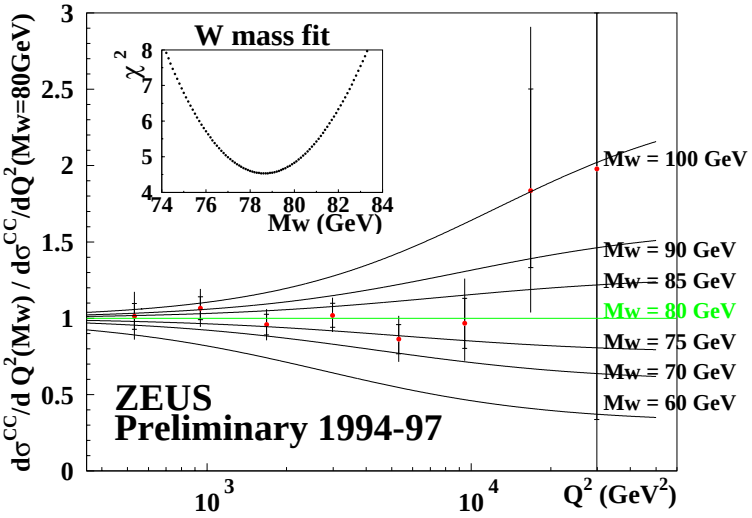

FIG. 10. Sensitivity of the CC cross section to the W mass, shown as a ratio of $d\sigma/dQ^2$ to the SM prediction, for several values of M_W between 60 and 100 GeV. The inlaid plot shows the χ^2 of the M_W fit.

V. CONCLUSIONS

The ZEUS neutral-current and charged-current DIS cross sections in the momentum transfer range $400 < Q^2 \lesssim 50000$ GeV^2, i.e., for Q^2 over more than two orders of magnitude, have been shown to be in good agreement with the

Standard Model predictions. However, a slight excess persists at highest Q^2. With the current data set, ZEUS has gained sensitivity to the electroweak propagator masses M_W and M_Z.

VI. OUTLOOK

In 1998, HERA switched from positron-proton collisions to electron-proton collisions. In addition, the proton energy was increased from 820 GeV to 920 GeV, thus increasing the center-of-mass energy by 6% from 300 GeV to 318 GeV. As of January 1, 1999, ZEUS had already accumulated 4.5pb^{-1} of e^-p data, nearly an order of magnitude more than accumulated during the only other e^-p running period 1992-1993. An additional $\sim 35\text{pb}^{-1}$ is expected in the 1999 calendar year. The HERA upgrade begins in May 2000, after which we foresee $\sim 150\text{pb}^{-1}$/year. These future data will improve our understanding of the electroweak interaction, and may even hold some surprises. We anticipate an exciting future for high-Q^2 physics at HERA.

ACKNOWLEDGMENTS

The kind assistance of my ZEUS colleagues in the preparation of this talk, and the great efforts of the conference organizers are greatly appreciated. This work is partly funded by the U.S. Department of Energy.

---

[1] ZEUS Collaboration, The ZEUS Detector Status Report, DESY 1993.
[2] A. Kwiatkowski, H. Spiesberger, and H.-J. Möhring, Comp. Phys. Commun. **69** (1992) 155;
A. Arbuzov et al., Comp. Phys. Commun. **94** (1996) 128.
[3] H.L. Lai, et al., Phys. Rev. D **55**, 1280, (,1997).
[4] M. Botje, DESY 99-038, NIKHEF 99-011 (in preparation).
[5] U.K. Yang and A. Bodek, Phys. Rev. Lett. 82 (1999) 2467.
[6] C. Caso et al., Eur. Phys. J. **C3** (1998) 1.